Evaluation of the Cooling Process of Thermal Storage Tanks with $LiNO_3$-$NaNO_3$-KNO_3 Ternary Mixture as Working Fluid for CSP Plants

Mauro Henríquez[1], Christian Suárez [2], Magin Mendoza[1], Abdiel Mallco[1], Mauricio Lague[1], Carlos Duran[1], Carlos Soto[1], Carlos Portillo[1], Javier Pino[2]

[1] Centro de Desarrollo Energético Antofagasta (CDEA)/Universidad de Antofagasta, Antofagasta, Chile

[2] Thermal Engineering Group, Energy Engineering Department, School of Engineering/Universidad de Sevilla, Sevilla, Spain.

Abstract

This research proposes the use of the mixture composed by 30%$LiNO_3$+57%KNO_3+13%$NaNO_3$ as thermal energy storage material in concentrated solar power plants due to its excellent thermal properties having a melting point of 127°C. The cooling process of the proposed ternary molten salt has been analyzed in a molten salt pilot plant built at the University of Antofagasta, which consists of a tank with a capacity of one ton, the controlled cooling tests were carried out from 400°C to 190°C. A computational fluid dynamics (CFD) model has been developed to analyze the transient cooling process of the molten salt tank, results were validated with the experimental data. The evolution of the temperature over time at all points in the tank has been obtained, the results show that the lowest temperatures are located near the free surface of the salts.

Keywords: Thermal Energy Storage; Lithium Nitrate; Concentrated Solar Power,

1. Introduction

Concentrating solar power, more commonly known as CSP, is unique among renewable energy generators because, although it is variable, like solar PV and wind, it can be easily coupled with thermal energy storage (TES) as well as conventional fuels, making it highly dispatchable (Kuravi et al., 2013). Concentrated solar power (CSP) technology with thermal energy storage (TES) can offer 24 h/day of operation at constant power (Wan et al., 2020), constituting an effective solution to the challenge of integrating renewable energy into the power system, as it provides renewable energy while bringing significant capacity, reliability and stability to the grid.

TES typically has lower capital costs than other storage technologies, as well as very high operational efficiency. The prototype TES system that was incorporated into the Solar Two project in Daggett, California, demonstrated a round-trip efficiency of over 97% (Pacheco et al., 2000), which was defined as the ratio of energy discharged to energy stored in the TES system. The thermal storage system of the above reference is a two-tank system designed to supply thermal energy at full steam generator output for three hours at the defined hot and cold salt temperatures of 565°C and 292°C, respectively (Kuravi et al., 2013). Two-tank molten salt thermal storage systems are considered the most mature thermal storage technology in solar thermal power plants (Zhang et al., 2020). In such system molten salts interact with the heat transfer fluid (HTF) of the solar field through a heat exchanger. During the day, the thermal energy from the solar field is used to maintain a steam turbine at full load and the rest of the solar field output is stored for later use. During cloud transients,

doi:10.18086/swc.2021.34.01 Available at http://proceedings.ises.org

the storage is discharged to keep it at full load until the clouds disappear. When the sun sets, the storage is fully discharged to produce during night-time periods (Suárez et al., 2015).

The most commonly used energy stored material in thermal solar plants is a binary salt, called "solar salt" consisting of a mixture of 60% $NaNO_3$ and 40% KNO_3 (Gil et al., 2010). However, the relatively high melting point of this mixture (221°C) represents a significant risk of local solidification in the operation of solar power plants during standby periods, making solar thermal plants have to work at a minimum operating temperature of 292°C.

Lithium nitrate is one of the most promising additives in TES materials under study for application in CSP plants (Fernández, Galleguillos, et al., 2014). In the last years, different authors (Cabeza et al., 2015; Cáceres et al., 2016; Fernández, Ushak, et al., 2014; Ushak et al., 2015) have investigated the most important thermal properties regarding the use of $LiNO_3$ as TES material in CSP plants. Lithium based salts have been studied for thermal energy storage (TES) applications due to their excellent thermophysical properties. The addition of lithium nitrate is assumed to improve the performance of molten salts, extending the work temperature range. All existing research regarding the use of a ternary mixture is done on a laboratory scale, and there is no test on a larger pilot scale or higher. The ternary mixture containing 30%$LiNO_3$+57%KNO_3+ 13%$NaNO_3$ has excellent thermal properties by having a heat capacity of 21% over solar salt, and a crystallization temperature of 127±5°C so it is considered a viable alternative as a TES material (Henríquez et al., 2020).

In the present work, experimental tests of the cooling process of the ternary mixture 30wt% $LiNO_3$ + 57wt% KNO_3+13wt% $NaNO_3$ were carried out inside the tank of the pilot plant of molten sales of the University of Antofagasta. These tests served to know the process of crystallization, solidification, as well as the distribution of temperatures, and the times of the different processes. On the other hand, the experimental study is complemented by a computational fluid dynamics (CFD) model for a molten salt tank working with the ternary mixture as working fluid.

2. Experimental

The ternary mixture 30 wt%$LiNO_3$+57 wt%KNO_3+13 wt%$NaNO_3$ used in the pilot-scale plant tests were prepared with nitrates salts $NaNO_3$ (99.5%) and KNO_3 (99.5%) both provided by the company SQM, and $LiNO_3$ (99%) from Todini Chemical. The tests for the ternary mixture were carried out in a stainless-steel grade 316L tank of 0.83 m^3 and 203 kg weight. The tank structure itself (1.2 m of internal diameter and 1.5 m of maximum height) is located over a refractory concrete base of 0.7 m thickness. Top and lateral walls of the tank are insulated with mineral wool (5 and 20 cm respectively) and the concrete base is insulated with foamglass (39 cm). The tank is partially filled with molten salt (34 cm of height), being the atmosphere air at ambient pressure. The tank was equipped with the commercial components detailed in Fig. 1, where four electric resistances of 1.2 kW provided the heat to melt the salt. The system contains 15 temperature sensors type PT100 class B 3-wire with 316-L stainless steel sheaths that are located inside and outside the tank. The sensors work in a temperature range of -200°C to 850°C (DIN 60751 specification) with an uncertainty of ±(0.3 + 0.005T).

A GVSO40/160A high-temperature vertical pump recirculated the fluid at a rate of 1 $m^3\ h^{-1}$. The plant incorporates a piping heating system with electric tracing. In order to monitor and control the different variables of the heating process, the plant uses a data acquisition and communication system, consisting of two data loggers, and an integrated Unitronics V570 programmable logic controller (PLC).

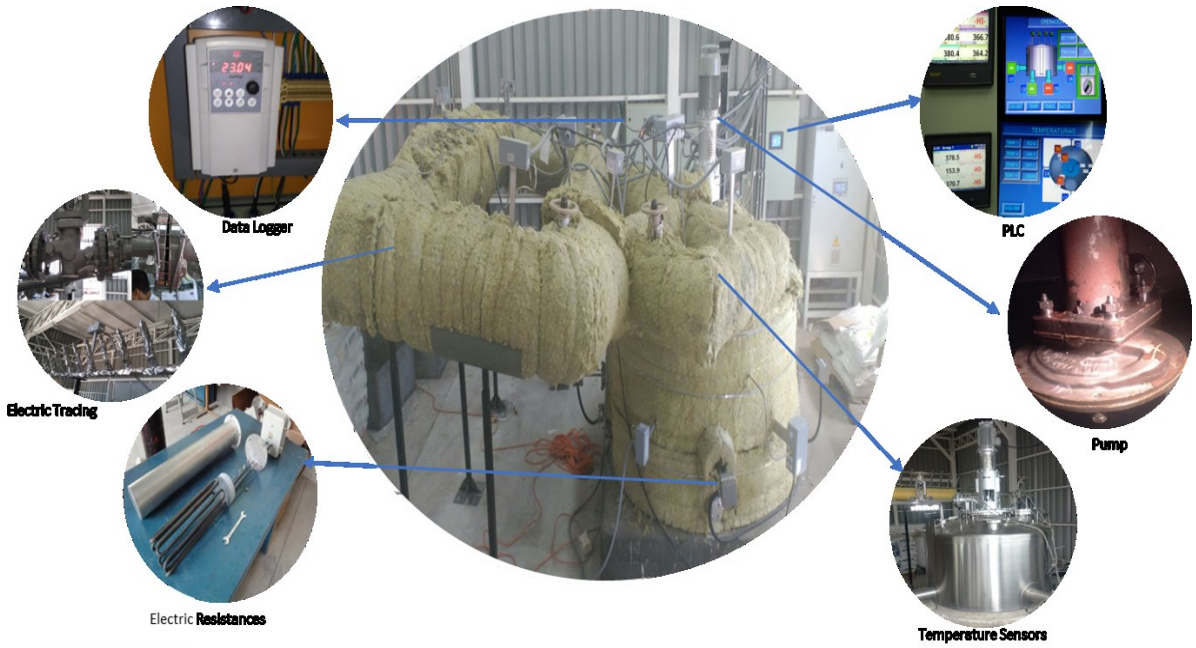

Fig. 1: Molten salt pilot plant at the University of Antofagasta

3. Results

3.1. Cooling from 400 ° C to 190 ° C

Next, the cooling process of the ternary mixture of 30% $LiNO_3$+57% KNO_3 +13% $NaNO_3$ in the molten salt tank of the pilot plant described above is described. During the cooling process of the ternary mixture of 30% $LiNO_3$+13%$NaNO_3$+57%KNO_3 in liquid phase from 400ºC to 190ºC. The molten salt was held at 400°C for a period of 12 h. Subsequently, the electrical resistances are turned off and it is allowed to cool naturally to room temperature. Once 190 ° C is reached, the temperature is maintained for a period of 24 hours.

As the temperature decreases from 400°C to 190°C, all the sensors immersed in the ternary salt inside the tank, offer a descending linear behavior without heating, observing stratification.

3.2. Crystallization process of the ternary mixture

After cooling tests up to 190 ° C, the system was allowed to cool until the material crystallized inside the salt tank. In Fig. 2 it is possible to observe the ternary mixture in the liquid phase, at a temperature of 190°C. According to the image it is possible to clearly observe the suction of the pump, and the metallic duct of stainless-steel pipe in which the electrical resistance is inserted, completely immersed in the fluid, which in its liquid phase has an appearance transparent similar to that of water.

Fig. 2: Cooling of the ternary mixture with 30% LiNO3 + 57% KNO3 + 13% NaNO3 inside the tank at a temperature of 190°C.

At 127°C some crystallized areas are around the suction of the pump and the metallic duct of the electrical resistance.

4. Numerical method section

CFD calculations have been performed using commercial software ANSYS FLUENT® (Launder B. E. & B., 2013) to analyse the transient evolution of temperatures during a stand-by cooling period in a molten salt storage tank. The main objective of the CFD simulations was to obtain an estimation of crystallization time. Molten salt temperature distribution and the regions in which crystallization occur first for different scenarios was also analysed. In a first CFD model, the methodology is validated using the experimental data for the pilot-scale storage tank and simulation results of different molten salt types were compared. Subsequently, a second CFD model was developed for a state-of-the-art storage tank of CSP plants and simulation results of different molten salt types were compared.

4.1. Problem definition and experimental validation of the numerical method

In this section, a description of the developed CFD model of the pilot-scale storage tank including geometry, mesh and boundary and initial conditions is presented. Experimental molten salt temperature results of the transient cooling process are used for the validation of the developed numerical method.

4.2. Geometry, boundary and initial conditions and materials thermophysical properties

A sketch of the pilot-scale storage tank is shown in Fig. 3. Taking advantage of the axial symmetry, a 2D axis-symmetric computational domain was adopted, obtaining a considerable reduction in terms of the mesh size and simulation time. The computational domain includes the molten salt (#1) and surrounding air (#2), mineral wool (#3) and foamglass (#4) insulations, a refractory concrete base (#5), a vertical pump (#6) located in the center-line of the tank and the stainless-steel tank structure (#7).

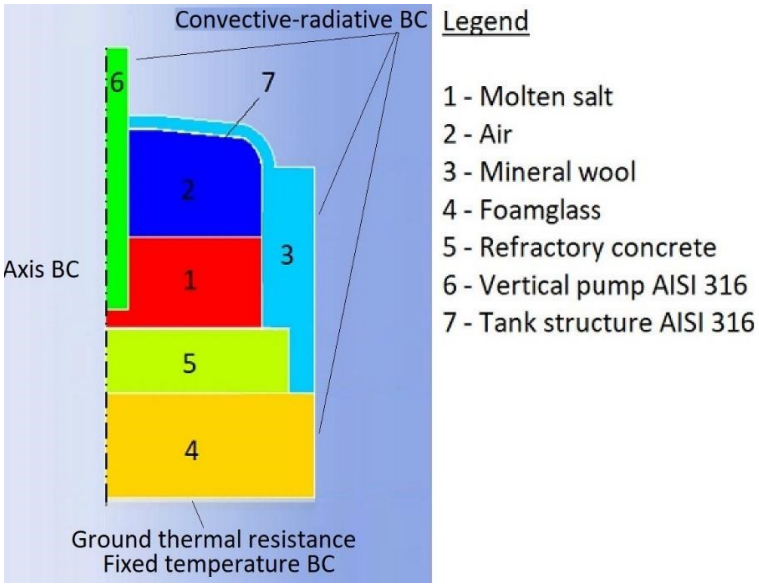

Fig. 3 – 2D axisymmetric pilot-scale tank computational domain and boundary conditions

The electrical resistances, which are off during the cooling process, are not considered in the computational domain.

The considered boundary conditions (BC's) of the problem were:

(i) axisymmetric BC in the tank centerline,

(ii) convective and radiative heat transfer BC at lateral and top walls in contact with exterior air at a constant temperature of 15ºC. External radiation effect is included in the selected value of the convective heat transfer coefficient h of 10 W/m^2K.

(iii) thermal resistance parameter with fixed temperature BC in the foamglass bottom to include the thermal insulation effect of the ground underneath the foamglass layer. This additional ground layer thermal resistance is computed as $\Delta y/k$ where Δy is the ground thickness and k is the ground thermal conductivity. A representative deep-ground constant temperature equal to the annual average temperature was specified at the outside wall surface. A sandy ground of 10 m thickness with a constant thermal conductivity of 2 W/mK was considered, with an external temperature of 15 ºC, representative for the annual average temperature of Antofagasta (Chile).

Materials initial temperatures were set according to the experimental data, starting with a molten salt temperature of 400 ºC. The rest of the initial temperatures were: stainless steel 385 ºC, rock wool 240 ºC, foamglass 165 ºC and concrete 360 ºC.

Materials thermophysical properties are summarized in tables 1 and 2 as a function of temperature for solids and fluids respectively .

Tab. 1: Temperature dependent thermophysical properties (solids). Property= $a_0 + a_1 \cdot T + a_2 \cdot T^2 + a_3 \cdot T^3$, T(ºC)

Material	ρ ($kg \cdot m^{-3}$)	Cp ($J \cdot kg^{-1} \cdot K^{-1}$)	λ ($W \cdot m^{-1} \cdot K^{-1}$)
Mineral wool	$a_0 = 20$	$a_0 = 871$	$a_0 = 3.49 \cdot 10^{-2}$, $a_1 = 9.62 \cdot 10^{-5}$,

			$a_2 = 1.47 \cdot 10^{-7}$, $a_3 = 4.21 \cdot 10^{-10}$
Foam glass	$a_0 = 20$	$a_0 = 871$	$a_0 = 3.76 \cdot 10^{-2}$, $a_1 = 2.53 \cdot 10^{-4}$, $a_2 = -3.29 \cdot 10^{-7}$, $a_3 = 6.75 \cdot 10^{-10}$
Concrete	$a_0 = 2250$	$a_0 = 750$, $a_1 = 0.75$	$a_0 = 1.70$
AISI 316	$a_0 = 7918$	$a_0 = 544$	$a_0 = 16.3$
Air	$a_0 = 1.18$, $a_1 = -2.65 \cdot 10^{-3}$ $a_2 = 2.50 \cdot 10^{-6}$,	$a_0 = 1006$	$a_0 = 1.52 \cdot 10^{-5}$, $a_1 = 8.49 \cdot 10^{-8}$ $a_2 = -2.18 \cdot 10^{-10}$, $a_3 = 2.85 \cdot 10^{-13}$

Tab 2. Temperature dependent thermophysical properties (fluids). Property= $a_0 + a_1 \cdot T + a_2 \cdot T^2 + a_3 \cdot T^3$, T (ºC)

Material	ρ (kg·m^{-3})	Cp (J·kg^{-1}·K^{-1})	μ (kg·m^{-1}·s^{-1})	λ (W·m^{-1}·K^{-1})
Solar salt	$a_0 = 2090$, $a_1 = -0.64$	$a_0 = 1443$, $a_1 = -0.17$	$a_0 = 5.50 \cdot 10^{-2}$, $a_1 = -4.35 \cdot 10^{-4}$ $a_2 = 1.22 \cdot 10^{-6}$, $a_3 = -1.16 \cdot 10^{-9}$	$a_0 = 0.45$
Ternary salt	$a_0 = 1803$, $a_1 = -0.50$	$a_0 = 1409$	$a_0 = 8.00 \cdot 10^{-2}$	$a_0 = 0.55$

4.3. Experimental validation

A validation of the numerical approach was performed by comparing the numerical predictions against the previously reported experimental results during the novel ternary molten salt cooling down. Experimental results were measured from an initial molten salt temperature of 400 ºC until a final secure operation limit temperature of the molten salt defined at 190 ºC. The variables compared in the validation are the transient temperature evolution of thermocouples located in the molten salt (sensor #6), interface wall tank-insulation (sensor #15), and interface bottom tank-concrete (sensor #11). Crystallization time is also a parameter of interest in the validation.

Validation results are shown in Fig. 4, including with dashed line the crystallization temperature of the molten salt (127 ºC) and an upper secure operation temperature limit (190 ºC). Results show a similar trend between the experimental and the simulated results for sensors #6, #11 and #15 with percentual temperature relative differences below 1.5 % in average and 4 % in the worst case. Higher temperature differences between the experimental results and the simulations were found during the initial time periods, due to the fact that initial temperature conditions are only known in a few points of the computational domain, being the rest of temperatures assumed. Simulation results also predict accurately the time in which the molten salt reach the temperature limit of 190 ºC, 70.9 h, in comparison with the experimental value of 71.8 h. Taking the temperature

limit as the reference, simulations prognosticated an extra period of 54.5 h before crystallization materialize at 127 ºC.

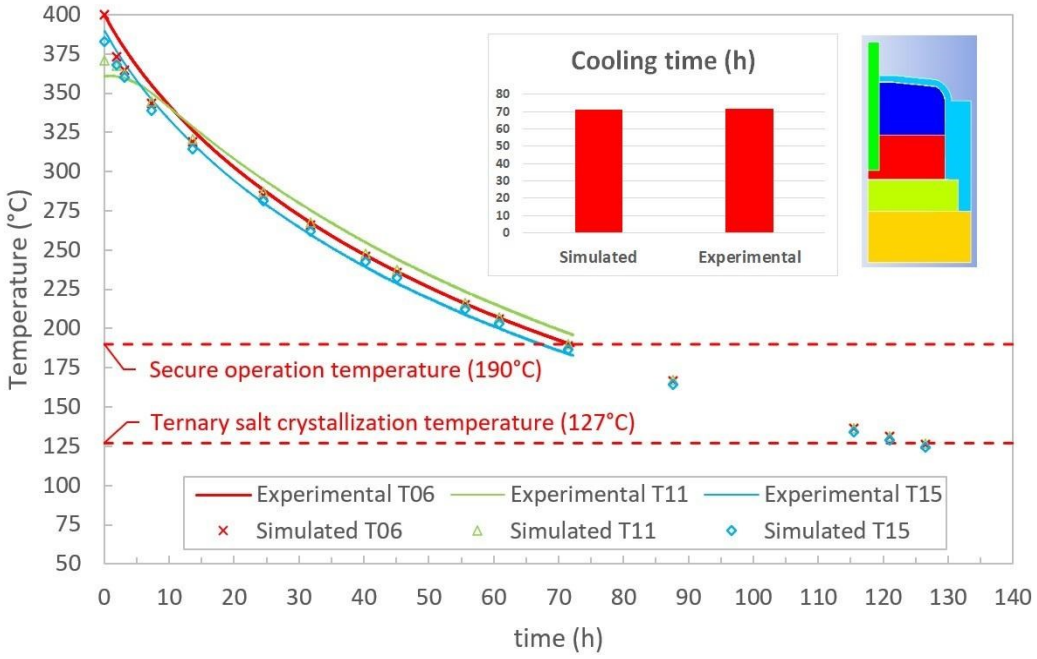

Fig. 4. Simulated results vs experimental results in the cooling down of the novel ternary molten salt.

5. Conclusions

The present work carried out at laboratory scale and in the pilot, plant confirms the excellent thermophysical properties that would allow Chilean lithium nitrate to be an option to replace the current solar salt, with a stable minimum operation temperature around 190 ºC.

CFD model of the pilot-scale tank was developed and validated with the experimental results in terms of the ternary mixture salt temperature evolution.

Percentual temperature relative differences were below 1.5 % in average and 4 % in the worst case.

The time elapsed experimentally of the ternary mixture cooling process from 400 to 190 ºC was 71.8 h, in good agreement with 70.9 h obtained with CFD simulations.

6. Acknowledgements

The authors would like to acknowledge the financial support provided by CONICYT / FONDAP 15110019 “Solar Energy Research Center" SERC-Chile. FIC-R 30413089 – 30488809 funded by Antofagasta Government. Scaling-UP Engineering 2030 UA-OTL Funds. VIU21P0051 Project National Research and Development Agency, Government of Chile

7. References

Cabeza, L. F., Gutierrez, A., Barreneche, C., Ushak, S., Fernández, Á. G., Inés Fernádez, A., & Grágeda, M., 2015. Lithium in thermal energy storage: A state-of-the-art review. Renewable and Sustainable Energy Reviews, 42, 1106–1112. https://doi.org/10.1016/j.rser.2014.10.096

Cáceres, G., Montané, M., Nasirov, S., & O'Ryan, R., 2016. Review of thermal materials for CSP plants and lcoe evaluation for performance improvement using chilean strategic minerals: Lithium salts and copper foams. Sustainability (Switzerland), 8(2). https://doi.org/10.3390/su8020106

Fernández, A. G., Galleguillos, H., & Pérez, F. J., 2014. Corrosion Ability of a Novel Heat Transfer Fluid for Energy Storage in CSP Plants. Oxidation of Metals, 82(5–6), 331–345. https://doi.org/10.1007/s11085-014-9494-3

Fernández, A. G., Ushak, S., Galleguillos, H., & Pérez, F. J., 2014. Development of new molten salts with LiNO3 and Ca(NO3)2 for energy storage in CSP plants. Applied Energy, 119(3), 131–140. https://doi.org/10.1016/j.apenergy.2013.12.061

Gil, A., Medrano, M., Martorell, I., Lázaro, A., Dolado, P., Zalba, B., & Cabeza, L. F., 2010. State of the art on high temperature thermal energy storage for power generation. Part 1-Concepts, materials and modellization. Renewable and Sustainable Energy Reviews, 14(1), 31–55. https://doi.org/10.1016/j.rser.2009.07.035

Henríquez, M., Guerreiro, L., Fernández, Á. G., & Fuentealba, E., 2020. Lithium nitrate purity influence assessment in ternary molten salts as thermal energy storage material for CSP plants. Renewable Energy, 149, 940–950. https://doi.org/10.1016/j.renene.2019.10.075

Kuravi, S., Trahan, J., Goswami, D. Y., Rahman, M. M., & Stefanakos, E. K., 2013. Thermal energy storage technologies and systems for concentrating solar power plants. Progress in Energy and Combustion Science, 39(4), 285–319. https://doi.org/10.1016/j.pecs.2013.02.001

Launder B. E., & B., S. D., 2013. ANSYS Fluent User' s Guide Releasde 15.0. Knowledge Creation Diffusion Utilization, 15317(November), 724–746.

Pacheco, J. E., Reilly, H. E., Kolb, G. J., & Tyner, C. E., 2000. Summary of the Solar Two test and evaluation program. Proceding of the Renewable Energy for the New Millenium, 1–11.

Suárez, C., Iranzo, A., Pino, F. J., & Guerra, J., 2015. Transient analysis of the cooling process of molten salt thermal storage tanks due to standby heat loss. Applied Energy, 142, 56–65. https://doi.org/10.1016/j.apenergy.2014.12.082

Ushak, S., Fernández, A. G., & Grageda, M., 2015. Using molten salts and other liquid sensible storage media in thermal energy storage (TES) systems. In Advances in Thermal Energy Storage Systems: Methods and Applications. Woodhead Publishing Limited. https://doi.org/10.1533/9781782420965.1.49

Wan, Z., Wei, J., Qaisrani, M. A., Fang, J., & Tu, N., 2020. Evaluation on thermal and mechanical performance of the hot tank in the two-tank molten salt heat storage system. Applied Thermal Engineering, 167(December 2019), 114775. https://doi.org/10.1016/j.applthermaleng.2019.114775

Zhang, X., Zhang, C., Wu, Y., & Lu, Y., 2020. Experimental research of high temperature dynamic corrosion characteristic of stainless steels in nitrate eutectic molten salt. Solar Energy, 209, 618–627. https://doi.org/10.1016/j.solener.2020.09.034